AAC Journals.ASM.org

Function of Cytochrome P450 Enzymes MycCI and MycG in *Micromonospora griseorubida*, a Producer of the Macrolide Antibiotic Mycinamicin

Yojiro Anzai,[a] Shu-ichi Tsukada,[a] Ayami Sakai,[a] Ryohei Masuda,[a] Chie Harada,[a] Ayaka Domeki,[a] Shengying Li,[b] Kenji Kinoshita,[c] David H. Sherman,[b] and Fumio Kato[a]

Faculty of Pharmaceutical Sciences, Toho University, Funabashi, Chiba, Japan[a]; Life Sciences Institute, Department of Medicinal Chemistry, Chemistry, and Microbiology and Immunology, University of Michigan, Ann Arbor, Michigan, USA[b]; and School of Pharmaceutical Sciences, Mukogawa Women's University, Nishinomiya, Hyogo, Japan[c]

The cytochrome P450 enzymes MycCI and MycG are encoded within the mycinamicin biosynthetic gene cluster and are involved in the biosynthesis of mycinamicin II (a 16-membered macrolide antibiotic produced by *Micromonospora griseorubida*). Based on recent enzymatic studies, MycCI is characterized as the C-21 methyl hydroxylase of mycinamicin VIII, while MycG is designated multifunctional P450, which catalyzes hydroxylation and also epoxidation at C-14 and C-12/13 on the macrolactone ring of mycinamicin. Here, we confirm the functions of MycCI and MycG in *M. griseorubida*. Protomycinolide IV and mycinamicin VIII accumulated in the culture broth of the *mycCI* disruption mutant; moreover, the *mycCI* gene fragment complemented the production of mycinamicin I and mycinamicin II, which are produced as major mycinamicins by the wild strain *M. griseorubida* A11725. The *mycG* disruption mutant did not produce mycinamicin I and mycinamicin II; however, mycinamicin IV accumulated in the culture broth. The *mycG* gene was located immediately downstream of the self-resistance gene *myrB*. The *mycG* gene under the control of *mycGp* complemented the production of mycinamicin I and mycinamicin II. Furthermore, the amount of mycinamicin II produced by the strain complemented with the *mycG* gene under the control of *myrBp* was approximately 2-fold higher than that produced by the wild strain. In *M. griseorubida*, MycG recognized mycinamicin IV, mycinamicin V, and also mycinamicin III as the substrates. Moreover, it catalyzed hydroxylation and also epoxidation at C-14 and C-12/13 on these intermediates. However, C-14 on mycinamicin I was not hydroxylated.

The cytochrome P450 enzymes (P450s) form a very large family of oxidative heme proteins, which are responsible for a diverse range of oxidative transformations across most life forms (12, 13). These reactions typically involve the modification of physiological and xenobiotic compounds and include the biosynthesis of various bioactive compounds (e.g., steroids, antibiotics, and signaling molecules). Approximately 40% of all known bacterial P450s are found in various species of the industrially important genus *Streptomyces*, which is the largest genus of the actinomycetes. Recent genome sequencing of the actinomycetes, particularly *Streptomyces*, has revealed an unexpectedly large number of genes encoding P450s (9, 16, 18, 24, 25). In secondary metabolic pathways, P450 genes are typically integrated within the biosynthetic cluster, where their products catalyze regiospecific and stereospecific oxidation of precursors. This results in structural diversity and also improved bioactivities of these molecules (21, 27). The P450s EryF (2) and EryK (30) are encoded within the erythromycin biosynthetic gene cluster and are involved in the biosynthesis of erythromycin A. Specifically, EryF catalyzes the hydroxylation of the macrolactone precursor 6-deoxyerthronolide B, while EryK catalyzes the formation of erythromycin D. As prototypic P450 hydroxylases involved in secondary metabolism, EryF and EryK exhibit strict substrate specificity. In contrast, PikC, which is involved in the methymycin/neomethymycin and pikromycin biosynthetic pathways of *Streptomyces venezuelae*, has broader substrate tolerance (33). This enzyme catalyzes the final hydroxylation step toward the 12-membered-ring macrolide YC-17 and also the 14-membered-ring macrolide narbomycin to produce methymycin/neomethymycin and pikromycin as major products. Recently, some P450 genes encoding multifunctional oxidation proteins have been identified in secondary metabolite biosynthetic clusters. For example, TamI, which is encoded within the tirandamycin biosynthetic gene cluster of *Streptomyces* sp. strain 307-9, has hydroxylation and also epoxidation functions (11). The enzyme is responsible for three hydroxylations and one epoxidation in the biosynthetic pathway from tirandamycin C to tirandamycin B. GfsF, which is involved in the biosynthetic pathway of *Streptomyces graminofaciens*, also has dual oxidation functions (20). This enzyme catalyzes stepwise epoxidation and hydroxylation during biosynthesis of the antibiotic FD-891.

Mycinamicin, which is produced by *Micromonospora griseorubida* A11725, is a 16-membered macrolide antibiotic with strong antibacterial activity against Gram-positive bacteria (29). Mycinamicin consists of a macrolactone substituted with two different sugars, desosamine and mycinose. The nucleotide sequence of the complete mycinamicin biosynthetic gene cluster has been documented, and 22 open reading frames (ORFs) including two putative cytochrome P450 enzyme genes, *mycCI* and *mycG*, were iden-

Received 3 November 2011 **Returned for modification** 11 December 2011
Accepted 25 April 2012
Published ahead of print 30 April 2012
Address correspondence to Yojiro Anzai, yanzai@phar.toho-u.ac.jp.
Supplemental material for this article may be found at http://aac.asm.org/.

doi:10.1128/AAC.06063-11

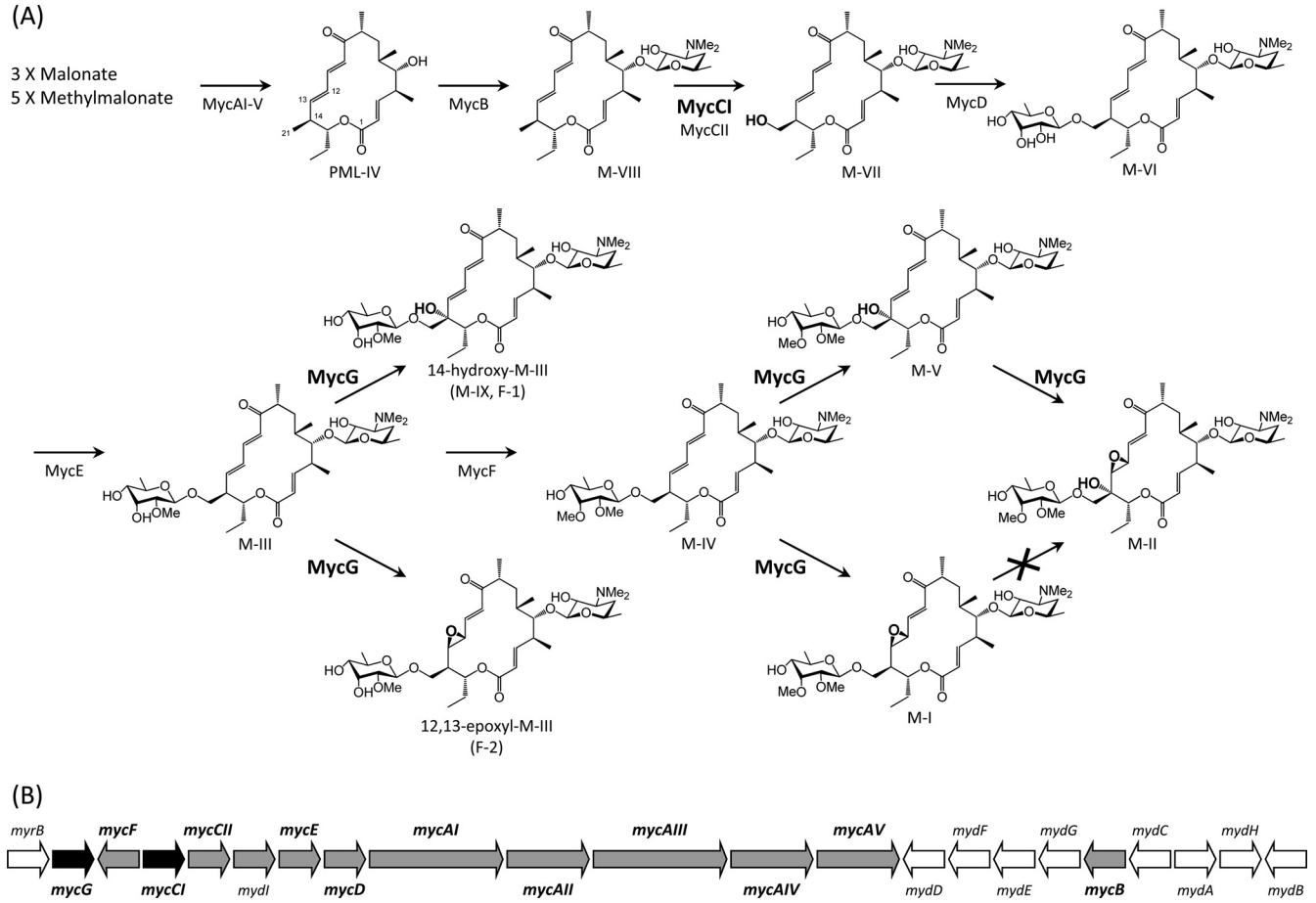

FIG 1 Mycinamicin biosynthetic pathway (A) and organization of mycinamicin biosynthetic gene cluster (B). The pathway from M-I to M-II is absent in *M. griseorubida* because there is no P450 enzyme which catalyzes hydroxylation at C-14 on M-I. Oxidative functionalities set up by cytochrome P450 enzymes are highlighted. Color codes in the *myc* gene cluster are as follows: black, cytochrome P450 genes; gray, mycinamicin biosynthetic genes shown in the biosynthetic pathway; and white, deoxysugar biosynthetic genes and the self-resistance gene. Me, methyl.

tified in the cluster as shown in Fig. 1 (5). MycCI is closely related to ChmHI (32) and TylHI (8), both of which are responsible for methyl group hydroxylations of 16-membered ring macrolides. *mycCI*, which is located adjacent to the *mycCII* encoding ferredoxin, is the first gene of a putative polycistronic operon consisting of 10 genes (*mycCI*, *mycCII*, *mydI*, *mycE*, *mycD*, *mycAI*, *mycAII*, *mycAIII*, *mycAIV*, and *mycAV*) in the mycinamicin biosynthetic gene cluster. In a recent *in vitro* study, we characterized MycCI as the C-21 methyl hydroxylase of mycinamicin VIII (M-VIII), which is the earliest macrolide form in the postpolyketide synthase (PKS) tailoring pathway. Moreover, we revealed that the optimal activity of MycCI is dependent on the native ferredoxin MycCII (4). Using purified MycG proteins overexpressed in *Escherichia coli* cells, we also characterized the *in vitro* functions of MycG (4). MycG monooxygenase is the first P450 to possess multiple oxidation functions; the enzyme recognized mycinamicin IV (M-IV) as an initial substrate and thereafter catalyzed sequential hydroxylation and epoxidation steps with M-IV or mycinamicin V (M-V) as the substrates to generate mycinamicin II (M-II). However, mycinamicin I (M-I), which was formed by the epoxidation of M-IV, was not recognized as a substrate by MycG. Inouye et al. showed by genetic complementation analysis of an M-IV accumulation mutant of *M. griseorubida* that a P450 enzyme encoded by the *mycG* gene catalyzed hydroxylation and also epoxidation at C-14 and C-12/13 on the macrolactone ring of mycinamicin, and they estimated that *M. griseorubida* A11725 possessed the ability to convert low levels of M-I to M-II (17). In the present study, we isolated *mycCI* and *mycG* disruption mutants and their respective gene complementation strains in order to confirm the functions of *mycCI* and *mycG* in the mycinamicin biosynthetic pathway. Using the *mycG* disruption mutant, we also investigated whether *M. griseorubida* possessed the ability to convert M-I to M-II.

We previously demonstrated that the purified MycG protein recognized the mycinamicin biosynthetic intermediates M-IV and mycinamicin III (M-III); moreover, their hydroxylation compounds, assumed to be mycinamicin XV (M-XV) and mycinamicin IX (M-IX), respectively, were detected in the reaction mixtures as minor peaks (4). During analysis of the mycinamicins produced by *mycE* and *mycF* disruption mutants, some of the mycinamicin VI (M-VI) and M-III derivatives oxidized by MycG were detected as minor peaks in the culture broth (31). In the present study, we confirmed that M-III (the precursor of M-IV in the mycinamicin biosynthetic pathway) is converted into C-14-hydroxy-M-III (M-IX) and C-12/13-epoxy-M-III by the P450 enzyme encoded by the *mycG* gene in *M. griseorubida*.

TABLE 1 Strains and plasmids used in this study

Strain or plasmid	Description or genotype[a]	Reference or Source
M. griseorubida		
A11725	Wild strain, mycinamicin producer	29
TPMA0016	Δ*mycF*, amino acids (aa) 2 to 253 replaced with FRT-*neo-oriT*-FRT-*attB* cassette	31
TPMA0023	Δ*mycCI*, aa 2 to 383 replaced with FRT-*oriT-neo*-FRT-*attB* cassette	This study
TPMA0025	Δ*mycG*, aa 2 to 398 replaced with FRT-*neo-oriT*-FRT-*attB* cassette	This study
TPMA0027	Δ*mycCI*, aa 2 to 383 replaced with FRT-*neo-oriT*-FRT-*attB* cassette	This study
TPMA0033	pMG517 including *mycCI* and *mycCII* induced into *mycCI* deletion mutant TPMA0023	This study
TPMA0034	pMG518 including *mycCI* induced into *mycCI* deletion mutant TPMA0023	This study
TPMA0040	Δ*mycF*, aa 2 to 253 replaced with FRT-*neo-oriT*-FRT-*attB* cassette; Δ*mycG*, aa 2 to 283 replaced with FRT-*aac(3)IV-oriT*-FRT-*attB* cassette	This study
TPMA0046	pMG519 including *myrB* and *mycG* induced into *mycG* deletion mutant TPMA0025	This study
TPMA0047	pMG520 including *mycG* induced into *mycG* deletion mutant TPMA0025	This study
TPMA0062	pMG521 including *mycG* controlled *myrB* promoter *myrBp* into *mycG* deletion mutant TPMA0025	This study
E. coli		
S17-1	Conjugation donor	American Type Culture Collection (ATCC)
BW25113	K-12 derivative, Δ*araBAD* Δ*rhaBAD*	14
JM109	General cloning host	TaKaRa, Japan
ATCC 25922	Test strain for antibacterial assay	ATCC
M. luteus		
ATCC 9341	Test strain for antibacterial assay	ATCC
S. aureus		
ATCC 25923	Test strain for antibacterial assay	ATCC
Plasmids		
pIJ790	λ-Red (*gam bet exo*) *cat araC rep101*(Ts)	14
pIJ773	Source of *aac(3)IV-oriT* for pMG510	14
pIJ776	Source of *neo-oriT* for pMG509	14
pLITMUS38	Cloning vector, *bla*	New England Biolabs
pUC19	Cloning vector, *bla*	TaKaRa, Japan
pDrive	TA cloning vector, *bla aph*	Qiagen
pSET152	*aac(3)IV*(Apr^r) *oriT attP int*	10
pSAN-lac	*bla tsr*	7
pETmycG-NH	MycG protein-coding region inserted into pET21b	4
pMR01	Cosmid clone containing some mycinamicin biosynthesis genes including *mycE* and *mycF*	5
pMG261	Cosmid clone containing some mycinamicin biosynthesis and self-resistance genes including *myrB*, *mycG*, and *mycF*	5
pMG501	1.5-kb FRT-*neo-oriT*-FRT-*attB* cassette inserted into pLITMUS38	31
pMG509	1.5-kb FRT-*oriT-neo*-FRT-*attB* cassette inserted into pLITMUS38	This study
pMG510	1.4-kb FRT-*aac(3)IV-oriT*-FRT-*attB* cassette inserted into pLITMUS38	This study
pMG511	8.8-kb BamHI fragment containing *mycCI* and *mycCII* inserted into pSAN-lac	This study
pMG512	9.2-kb EcoRI-HindIII fragment containing *myrB*, *mycG*, and *mycF* inserted into pSAN-lac	This study
pMG513	*mycCI* replaced with FRT-*neo-oriT*-FRT-*attB* cassette on pMG511	This study
pMG514	*mycCI* replaced with FRT-*oriT-neo*-FRT-*attB* cassette on pMG511	This study
pMG515	*mycG* replaced with FRT-*neo-oriT*-FRT-*attB* cassette on pMG512	This study
pMG516	5′-end region of *mycG* replaced with FRT-*aac(3)IV-oriT*-FRT-*attB* cassette on pMG512	This study
pMG517	2.0-kb SphI-HindIII fragment including *mycCI* and *mycCII* inserted into pSET152	This study
pMG518	1.8-kb SphI-KasI fragment including *mycCI* inserted into pSET152	This study
pMG519	3.5-kb NotI-NruI fragment including *myrB* and *mycG* inserted into pSET152	This study
pMG520	2.2-kb ApaLI-NruI fragment including *mycG* inserted into pSET152	This study
pMG521	*mycG* controlled *myrB* promoter *myrBp* inserted into pSET152	This study

[a] FRT, FLP recombination target.

MATERIALS AND METHODS

Strains, media, and culture conditions. The strains used in this study are shown in Table 1. The culture conditions for *M. griseorubida* and *E. coli* were as described previously (31).

Vectors, DNA manipulation, and PCR. The vectors and PCR primers used in this study are shown in Table 1 and Table S1 in the supplemental material, respectively. TaKaRa *Ex Taq* (TaKaRa, Japan), KOD FX (Toyobo, Japan), and PfuTurbo (Stratagene) DNA polymerases were used for amplification of DNA fragments by PCR. Plasmid and genomic DNA amplification, restriction enzyme digestion, fragment isolation, cloning, and DNA fragment amplification were performed according to standard procedures. Southern blot analysis was performed as described in our previous study (31).

Construction of the gene disruption cassettes FRT-*oriT*-*neo*-FRT-*attB* and FRT-*aac(3)IV*-*oriT*-FRT-*attB*. The orientation of the resistance *oriT* fragment on pMG509, which contained gene disruption cassette FRT-*oriT*-*neo*-FRT-*attB*, was opposite that on pMG501. To construct pMG509, the 1.3-kb XbaI fragment including *neo* and *oriT* derived from pIJ776 was ligated with the 2.9-kb XbaI fragment derived from pMG501. The 1.3-kb XbaI fragment including *aac(3)IV* and *oriT* derived from pIJ773 was ligated with the 2.9-kb XbaI fragment derived from pMG501 to construct pMG510 containing gene disruption cassette FRT-*aac(3)IV*-*oriT*-FRT-*attB*. The resulting plasmids, pMG509 and pMG510, were digested with several restriction enzymes to confirm the direction of *neo*-*oriT* and *aac(3)IV*-*oriT* in these disruption cassettes.

Construction of plasmids. The *mycCI*-disrupted plasmids, pMG513 and pMG514, were constructed using the λ-Red-mediated recombination system as described in our previous study (31). To construct pMG511, the 8.8-kb BamHI fragment containing *mycCI* and *mycCII* derived from pMR01, which was selected from the *M. griseorubida* A11725 genomic DNA library constructed with the cosmid vector pKC505 (26), was cloned into pSAN-lac. pKC505 possesses the apramycin resistance gene *aac(3)IV* as a marker. The disruption cassettes FRT-*neo*-*oriT*-FRT-*attB* and FRT-*oriT*-*neo*-FRT-*attB* were amplified by PCR with the primers DmycCIF and DmycCIR using the 1.5-kb EcoRV fragments from pMG501 and pMG509, respectively. *E. coli* BW25113/pIJ790 cells containing pMG511 were transformed with the amplified cassettes by electroporation. The resulting transformants were characterized by PCR with a set of oligonucleotides (RecognitionDmycCIF and RecognitionDmycCIR) priming outside the recombination region, and the resulting plasmids, pMG513 and pMG514, were used for disruption of the *mycCI* gene.

The *mycG*-disrupted plasmids, pMG515 and pMG516, were also constructed using the λ-Red-mediated recombination system. The 9.2-kb EcoRI-HindIII fragment containing *myrB*, *mycG*, and *mycF* derived from pMR261 was cloned into pSAN-lac to construct pMG512. To generate pMG515, the complete *mycG* region on pMG512 was replaced with the disruption cassette FRT-*neo*-*oriT*-FRT-*attB*, which was amplified with the primers DmycGF and DmycGR1 using the 1.5-kb EcoRV fragment from pMG501as the template. To generate pMG516, the 5′-end region of *mycG* on pMG512 was replaced with the disruption cassette FRT-*aac(3)IV*-*oriT*-FRT-*attB*, which was amplified with the primers DmycGF and DmycGR2 using the 1.4-kb EcoRV fragment from pMG510 as the template.

pMG517 and pMG518 were constructed to perform the genetic complementation studies for the *mycCI* disruption mutant. The 2.0-kb DNA fragment possessing the *mycCI* and *mycCII* clusters including the *mycCI* promoter region was amplified by PCR with the primers mycCIproF and mycCIIR. The 2.0-kb PCR product digested with SphI and HindIII was cloned into pUC19. After confirming the sequence of the cloned fragment, the SphI-HindIII fragment from the recombinant plasmid was blunted and inserted into the EcoRV site on pSET152 to generate pMG517. To construct pMG518 including the *mycCI* promoter and MycCI protein-coding region, the 1.8-kb SphI-KasI fragment from the cloned SphI-HindIII fragment was also blunted and inserted into the EcoRV site on pSET152.

For genetic complementation, studies with the *mycG* disruption mutant, pMG519, pMG520, and pMG521 were constructed. The 3.5-kb NotI-NruI and 2.2-kb ApaLI-NruI fragments from pMG512 were blunted and inserted into the EcoRV site on pSET152 to generate pMG519 containing the region from the *myrB* promoter to the *mycG* gene and pMG520 containing the region from the 3′end of *myrB* to *mycG*, respectively. The *myrB* gene promoter region, *myrBp*, was amplified by PCR with the primers myrBpF and myrBpR. The 0.7-kb PCR product digested with HindIII was cloned into pLITMUS38. After confirming the sequence of the cloned fragment, the 0.7-kb HindIII-NdeI fragment from the clone and the 1.2-kb NdeI-HindIII MycG protein-coding fragment, which was obtained from pETmycG-NH (4), were ligated with T4 DNA ligase, and then these ligated DNA fragments were digested with HindIII. The 1.9-kb HindIII fragment containing *myrBp* and *mycG* was blunted and inserted into the EcoRV site on pSET152 to generate pMG521.

Conjugation procedure. The intergeneric conjugation from *E. coli* S17-1 to *M. griseorubida* was performed as described in our previous study (31). The genetic characteristics of the exconjugants, which were screened for resistance to the antibiotics used as recombination markers, were confirmed by PCR and Southern hybridization as described in our previous study (31).

Analysis of mycinamicins in the *M. griseorubida* culture. To determine the mycinamicin production levels, *M. griseorubida* was cultured in 5 ml of MR0.1S broth with the appropriate antibiotics on a rotary shaker (150 rpm) at 27°C for 7 to 10 days. The broth was adjusted to a pH of 9 to 11 with 28% ammonia solution and extracted with an equal volume of ethyl acetate (EtOAc).

Intermediate feeding into the *M. griseorubida* culture plate and sample preparation for high-performance liquid chromatography (HPLC) analysis were performed using a protocol modified from our previous study (3). A seed culture was grown in 5 ml of MR0.1S broth for 5 days, and 150 μl of this seed culture was then spread on agar plates containing 15 ml of MR0.1S. Next, 1 ml of mycinamicin biosynthetic intermediate (500 μg) in 30% dimethyl sulfoxide-water was overlaid on the agar plate seed culture. After 8 days, the agar was homogenized and extracted with a 2-fold volume of EtOAc containing 1% triethylamine at 50°C; the extract was then concentrated *in vacuo*.

An equal volume of 0.1% trifluoroacetic acid (TFA) was added to the organic layer or the EtOAc solution to dissolve the crude extracts. The water layer containing mycinamicins was adjusted to a pH of 9 to 11 with 28% ammonia solution and extracted with an equal volume of EtOAc. The organic layer was concentrated *in vacuo*, and each residue was dissolved in methanol for HPLC analyses with a diode array detector model L-2450 (Hitachi, Japan) and liquid chromatography-mass spectrometry (LC-MS) analyses with a liquid chromatograph mass spectrometer model LCMS2010 (Shimadzu, Japan).

Fermentation, isolation, and identification of compounds F-1 and F-2. *M. griseorubida* TPMA0016 was cultured in 300-ml Erlenmeyer flasks containing 50 ml of MR0.1S broth. The flasks were incubated on a rotary shaker (120 rpm) at 27°C for 3 to 5 days. Next, 3-ml aliquots of the culture were transferred into each of 10 500-ml Sakaguchi flasks, containing 300 ml of FMM medium; these flasks were incubated on a rotary shaker (120 rpm) at 27°C for 11 days. The broth filtrate was adjusted to a pH of 9 to 11 with 28% ammonia solution and extracted with EtOAc. Next, the mycelium was extracted with EtOAc containing 1% triethylamine, and the extract was concentrated *in vacuo*. The combined crude extracts were dissolved with EtOAc, after which an equal volume of 0.1% TFA was added. The water layer containing mycinamicins was adjusted to a pH of 9 to 11 with 28% ammonia solution and extracted with an equal volume of EtOAc. After concentrating the organic layer *in vacuo*, the extracts were applied to a silica gel column (22 cm by 3 cm, silica gel 60; Merck) and eluted with a chloroform–methanol–28% ammonia solution (100:10:1). The fractions containing antibacterial metabolites were applied to a preparative HPLC system with a column Shim-pack PREP-ODS (inside diameter of 250 mm by 20 mm; Shimadzu, Japan) using the mobile phases acetonitrile (MeCN)–0.06% TFA (35:65) (flow rate, 10 ml/min) or MeCN–0.06% TFA (25:75) (flow rate, 20 ml/min) for collecting F-1 or F-2, respectively. Each fraction, which contained F-1 or F-2, was adjusted to a pH of 9 to 11 with 28% ammonia solution, and the fractions were then extracted with an equal volume of EtOAc. After concentrating the organic solution to dryness *in vacuo*, F-1 (12.6 mg) and F-2 (10.9 mg) were obtained. The purified F-1 and F-2 were characterized by ^{1}H nuclear magnetic resonance (^{1}H NMR; 600 MHz) and ^{13}C NMR (150 MHz) spectroscopy (JEOL JNM-ECA600). The ^{1}H NMR and ^{13}C NMR spectra of the products were assigned by a combination of ^{1}H-^{1}H correlation spectroscopy (COSY), distortionless enhancement by polarization transfer (DEPT) spectroscopy, and ^{1}H-^{13}C heteronuclear correlation spectros-

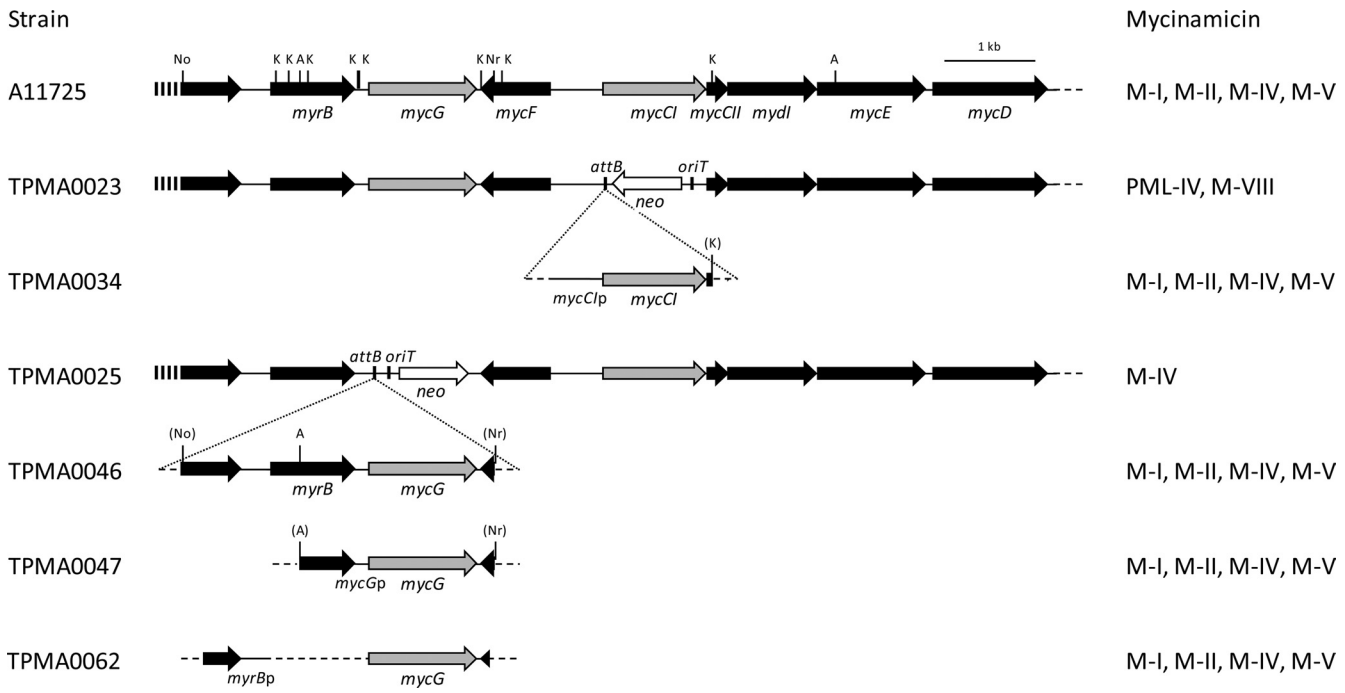

FIG 2 Physical maps of the region, including *mycCI*, *mycG*, and the flanking genes of the wild strain *Micromonospora griseorubida* A11725, *mycCI* disruption mutant TPMA0023, and *mycG* disruption mutant TPMA0025 and the DNA fragments introduced into these disruption mutants for the gene complementation study. The major mycinamicins in the culture broth of the wild strain, disruption mutants, and respective complementation strains (TPMA0034, *mycCI*; TPMA0046, TPMA0047, and TPMA0062, *mycG*) were detected with high-performance liquid chromatography (HPLC) (see Fig. S2 and S4 in the supplemental material). The relevant restriction sites are indicated as follows: A, ApaLI; K, KasI; No, NotI; and Nr, NruI. Mycinamicins in the ethyl acetate (EtOAc) extracts from the culture broth were analyzed with HPLC. Trace amounts of M-IV and M-V were detected in strains A11725, TPMA0034, TPMA0046, TPMA0047, and TPMA0062.

copy (HETCOSY) and compared with those of other mycinamicins (15, 19).

Antibacterial activity. Antibacterial activities were determined by microbroth dilution method using Mueller-Hinton medium (Becton, Dickinson and Company) (6). After the addition of test compounds, Gram-positive bacteria *Staphylococcus aureus* ATCC 25923 and *Micrococcus luteus* ATCC 9341 and the Gram-negative bacterium *E. coli* ATCC 25922 were grown at 37°C for 20 to 24 h. MICs were defined as the lowest concentration in which an 80% inhibition of growth was observed.

RESULTS AND DISCUSSION

Functions of the *mycCI* and *mycG* genes in *M. griseorubida*. In this study, isolation of gene disruption mutants was performed with disruption cassettes containing a bacteriophage ϕC31 *attB* attachment site from *Streptomyces lividans* (28) as described in our previous study (31). The plasmid pMG514, in which the protein-coding region of *mycCI* on pMG511 was replaced with the disruption cassette FRT-*oriT*-*neo*-FRT-*attB*, was introduced into strain A11725 by intergeneric conjugation. The neomycin-resistant (Neo^r) and thiostrepton-sensitive (Thio^s) transconjugant TPMA0023 was subjected to PCR to confirm that the chromosomal copy of A11725 *mycCI* was deleted by double crossover (data not shown). Moreover, the deletion of the *mycCI* gene in strain TPMA0023 was confirmed by Southern blot analysis (data not shown). The *mycCI* disruption mutant TPMA0023 did not produce M-I and M-II, which were major products of the wild strain A11725, when cultured in MR0.1S broth; however, protomycinolide IV (PML-IV) and M-VIII were detected in the EtOAc extract from the culture broth (Fig. 2; see also Fig. S1 in the supplemental material). For genetic complementation of the *mycCI* disruption mutant TPMA0023, pMG518 including *mycCI* was transferred to TPMA0023 by intergeneric conjugation. The transconjugant TPMA0034, isolated from the conjugation plate containing apramycin and nalidixic acid, produced M-I and M-II as major products (Fig. 2; see also Fig. S1 in the supplemental material). The amount of M-II produced by TPMA0034 was approximately 66% of that produced by the wild strain A11725. Insertion of pMG518 into the portable *attB* site on the chromosome of TPMA0034 was confirmed by Southern blot analysis (data not shown); moreover, PCR was performed with several primer pairs for TPMA0034 to confirm that the *mycCI* gene was inserted into the chromosome by site-specific recombination between the portable *attB* site on the chromosome and the *attP* site on pMG518 (data not shown). In this study, we isolated another *mycCI* disruption mutant, TPMA0027, in which the direction of the *neo* gene was the same as that of the mycinose biosynthesis gene cluster. However, the total amounts of PML-IV and M-VIII in the culture broth of TPMA0027 were lower than those in the culture broth of TPMA0023, in which the direction of the *neo* gene in the disruption cassette was opposite that of the mycinose biosynthesis genes in the mycinamicin biosynthetic gene cluster (data not shown); therefore, it was concluded that the direction of the *neo* gene transcription exerted a negative effect for mycinamicin productivity. Indeed, such a relationship between the direction of a replaced gene and the productivity of mycinamicin biosynthetic intermediates was previously observed in *mycE* disruption mutants (31).

To isolate the *mycG* disruption mutant, pMG515, on which the complete *mycG* region was replaced with the disruption cassette FRT-*oriT*-*neo*-FRT-*attB*, was introduced into strain A11725 by intergeneric conjugation. The resulting transconjugant TPMA0025 (Neo^r, Thio^s) was subjected to Southern blot analysis to confirm that the *mycG* gene was deleted from the chromosomal DNA from A11725 (data not shown). Moreover, deletion of the *mycG* gene by double crossover between the pMG515 and A11725 chromosomes was confirmed by PCR (data not shown). When the *mycG* disruption mutant TPMA0025 was cultured in MR0.1S broth, M-I, M-II, and M-V were not detected in the EtOAc extract; however, M-IV did accumulate in the culture broth (Fig. 2; see also Fig. S2 in the supplemental material). The *mycG* gene was located immediately downstream of *myrB*, encoding 23S rRNA methyltransferase for self-resistance, and there were at least two promoters, *mycGp* and *myrBp*, which would be able to control the expression of *mycG*. A 2.7-kb fragment including the MycG protein-coding region and *mycGp* previously restored M-I and M-II production of the M-IV accumulation mutant, which was obtained with *N*-methyl-*N*′-nitro-*N*-nitrosoguanidine treatment (17). However, it was assumed that the promoter *myrBp*, which is located immediately upstream of *myrB*, could also control the expression of *mycG*. For the genetic complementation of the *mycG* disruption mutant TPMA0025, three kinds of plasmids—pMG519, pMG520, and pMG521—were constructed. pMG519 possessed the *myrBp* and *mycGp* regions upstream of *mycG*, and therefore, the expression of *mycG* on this plasmid could be controlled by *myrBp* and/or *mycGp*. In pMG520, a 2.2-kb DNA fragment, which included the region from the 3′ end of *myrB* to *mycG*, was inserted; the expression of *mycG* on this plasmid was controlled by *mycGp*. The *mycG* complementation plasmids pMG519 and pMG520 were introduced into the *mycG* disruption mutant TPMA0025. The resulting transconjugants, TPMA0046 and TPMA0047, produced M-II (5.2 μg/ml and 4.1 μg/ml, respectively). The amount of M-II produced by TPMA0046 and TPMA0047 was almost the same as that produced by the wild strain A11725 (4.4 μg/ml) (Fig. 2; see also Fig. S2). Moreover, M-I and M-V production by these complementation strains was restored (Fig. 2; see also Fig. S2). Insertion of the complementation plasmids into the portable *attB* site on the chromosome of the respective gene complementation strains was confirmed by Southern blot analysis (data not shown); the size of the complementation DNA fragments inserted into the chromosomes of these complementation strains was confirmed by PCR (data not shown). On the *mycG* complementation plasmid pMG521, the open reading frame of *mycG* was directly attached to the amplified *myrBp* region. The nucleotide sequence of the 1.9-kb HindIII fragment containing *myrBp* and *mycG* on pMG521 was identified to be the same as that of the wild strain A11725 except for the connection site NdeI between the *myrBp* and *mycG* regions. The transconjugant TPMA0062 produced M-II (9.3 μg/ml); the amount was approximately 2-fold higher than that produced by the wild strain A11725. Moreover, M-I and M-V productivities by TPMA0062 were higher than that of A11725. The insertion of this complementation plasmid into the portable *attB* site and the size of the complementation DNA fragment inserted into the chromosome were confirmed by Southern blot analysis and PCR, respectively (data not shown). We hypothesize that the transcription of *mycG* is driven by these two promoters, *myrBp* and *mycGp*. It is interesting to speculate which promoter is the main regulator of *mycG* expression during mycinamicin biosynthesis, and in our future studies, we should investigate which promoter mainly controls the transcription of *mycG* by performing experiments such as Northern blotting, reverse transcriptase (RT)-PCR, and S1 nuclease mapping.

Multifunctional P450 enzyme MycG in mycinamicin producer. The *mycG* disruption mutant TPMA0025 did not produce M-I, M-II, and M-V, and the mycinamicin biosynthetic intermediate M-IV accumulated in the culture broth. In our previous enzymatic study, the cytochrome P450 protein MycG catalyzed hydroxylation and also epoxidation at C-14 and C-12/13 on the macrolactone ring of mycinamicin. In particular, M-IV was an initial substrate of MycG; moreover, MycG converted M-IV into M-V and M-I and M-V into M-II. However, M-I was not recognized as a substrate by MycG and was not converted into M-II (3). On the other hand, it was proposed by Inouye et al. that *M. griseorubida* A11725 possessed the ability of low-level conversion from M-I to M-II (17). Therefore, to confirm M-I hydroxylation reaction in *M. griseorubida*, a bioconversion study for mycinamicin biosynthetic intermediates was performed by using the *mycG* disruption mutant TPMA0025 and the PKS gene *mycAV* disruption mutant M7A21 (3) (Fig. 3). The intermediates PML-IV, M-IV, M-V, and M-I were added individually into plate cultures of TPMA0025 and M7A21, and the culture plates were incubated at 27°C for 8 days. PML-IV was converted into M-IV by TPMA0025 as would be expected according to the biosynthetic pathway shown in Fig. 1A. In contrast, M-IV, M-V, and M-I were not converted into any other intermediates because of the loss of MycG activity in TPMA0025. On the other hand, M7A21, which retained its MycG activity, converted M-IV into M-II and M-I and M-V into M-II; however, it did not convert M-I into M-II (Fig. 1A). These results indicated that M-I was not converted into M-II by *M. griseorubida* but was a shunt metabolite in mycinamicin biosynthesis.

In our previous enzymatic study, MycG recognized M-IV as an initial substrate. Moreover, mycinose at C-21 of the mycinamicin macrolactone ring was required for efficient catalysis by MycG (4). Mycinose in M-IV was generated from 6-deoxyallose via javose by two *O*-methyltransferases, MycE and MycF (22). The MycF protein catalyzes methylation at the C3″-OH group of javose in M-III. In a recent study, we observed that M-III (C3″-demethyl M-IV) accumulated in the culture broth of the *mycF* disruption mutants TPMA0004 and TPMA0016; furthermore, two unknown metabolites, F-1 and F-2, which were assumed to be hydroxylated and epoxidized M-IIIs, respectively, were detected in the EtOAc extracts of the mutants (31). We postulated that the hydroxylation and epoxidation of M-III were catalyzed by the P450 protein MycG in *M. griseorubida*. Thus, we isolated the *mycF* and *mycG* double-disruption mutant and identified the structure of the metabolites F-1 and F-2. To generate the *mycG* disruption plasmid pMG516, the 5′-end region of *mycG* on pMG512 was replaced with the disruption cassette FRT-*aac(3)IV*-*oriT*-FRT-*attB*. pMG516 was introduced into the *mycF* disruption mutant TPMA0016, and partial deletion of *mycG* on the chromosome in the resulting transconjugant TPMA0040 (Apr^r Neo^r) was confirmed by PCR (data not shown). The *mycF* and *mycG* double-disruption mutant TPMA0040 accumulated M-III and M-VI in the culture broth; however, F-1 and F-2, which were produced by TPMA0016, were not detected in the EtOAc extract from the culture broth of TPMA0040 (Fig. 4).

F-1 and F-2 were isolated and purified from 3.0 liters of

(A)

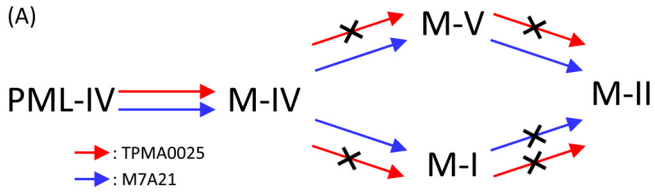

(B)

Strain	Intermediate	Mycinamicin
TPMA0025 (Δ*mycG*)	PML-IV	M-IV
	M-IV	M-IV
	M-V	M-I, M-V
	M-I	M-IV, M-I
	None	M-IV
M7A21 (Δ*mycAV*)	PML-IV	M-II, M-I
	M-IV	M-II, M-I, M-IV
	M-V	M-II
	M-I	M-I
	None	–

(C)

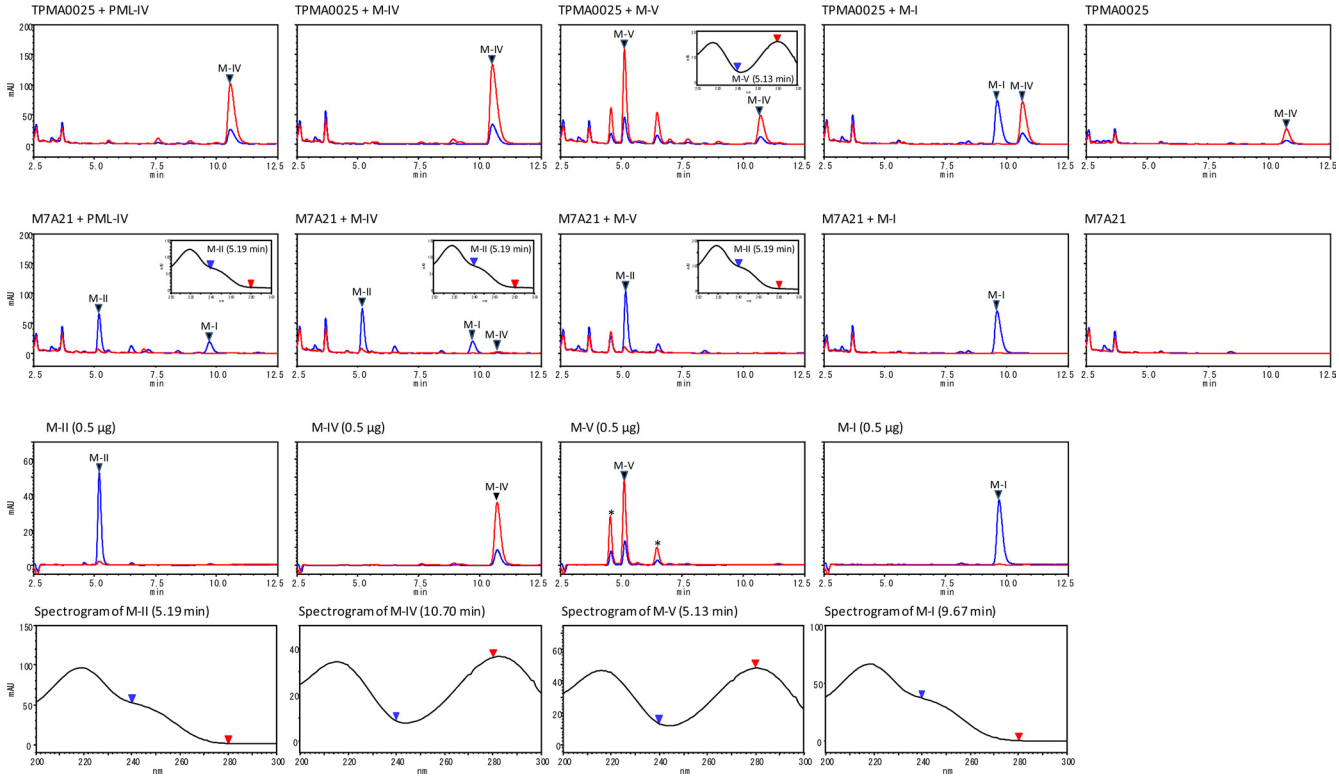

FIG 3 (A) Mycinamicin biosynthetic pathway of the *mycG* disruption mutant TPMA0025 and the *mycAV* disruption mutant M7A21 based on a bioconversion study of mycinamicin biosynthetic intermediates (B). The crossed arrows in panel A represent the undetected pathways in the mutants. (B) Bioconversion of mycinamicin biosynthetic intermediates by TPMA0025 and M7A21. Mycinamicin intermediates (500 μg) were added to culture plates of TPMA0025 and M7A21, and the culture plates were incubated at 27°C for 8 days. Mycinamicins in the ethyl acetate (EtOAc) extracts from the culture plates fed mycinamicin biosynthetic intermediates were analyzed with HPLC culture plate fed M-IV (C). Trace amounts of M-IV were detected in M7A21 culture plate fed M-IV. (C) HPLC chromatograms of the EtOAc extract obtained from culture plates fed with mycinamicin intermediates (PML-IV, M-IV, M-V, and M-I) of TPMA0025 and M7A21 and UV spectrograms of M-II and M-V detected in the EtOAc extract. HPLC chromatograms of the mycinamicin intermediates are shown with UV spectrograms. The purity of M-V was approximately 70%; other compounds included in the M-V powder are shown with asterisks. HPLC conditions: column, ODS-80Tm (Tosoh); mobile phase, MeCN, 0.06% TFA (35:65); flow rate, 0.8 ml/min; UV wavelength, 200 to 300 nm. Blue line, at 240 nm; red line, at 280 nm.

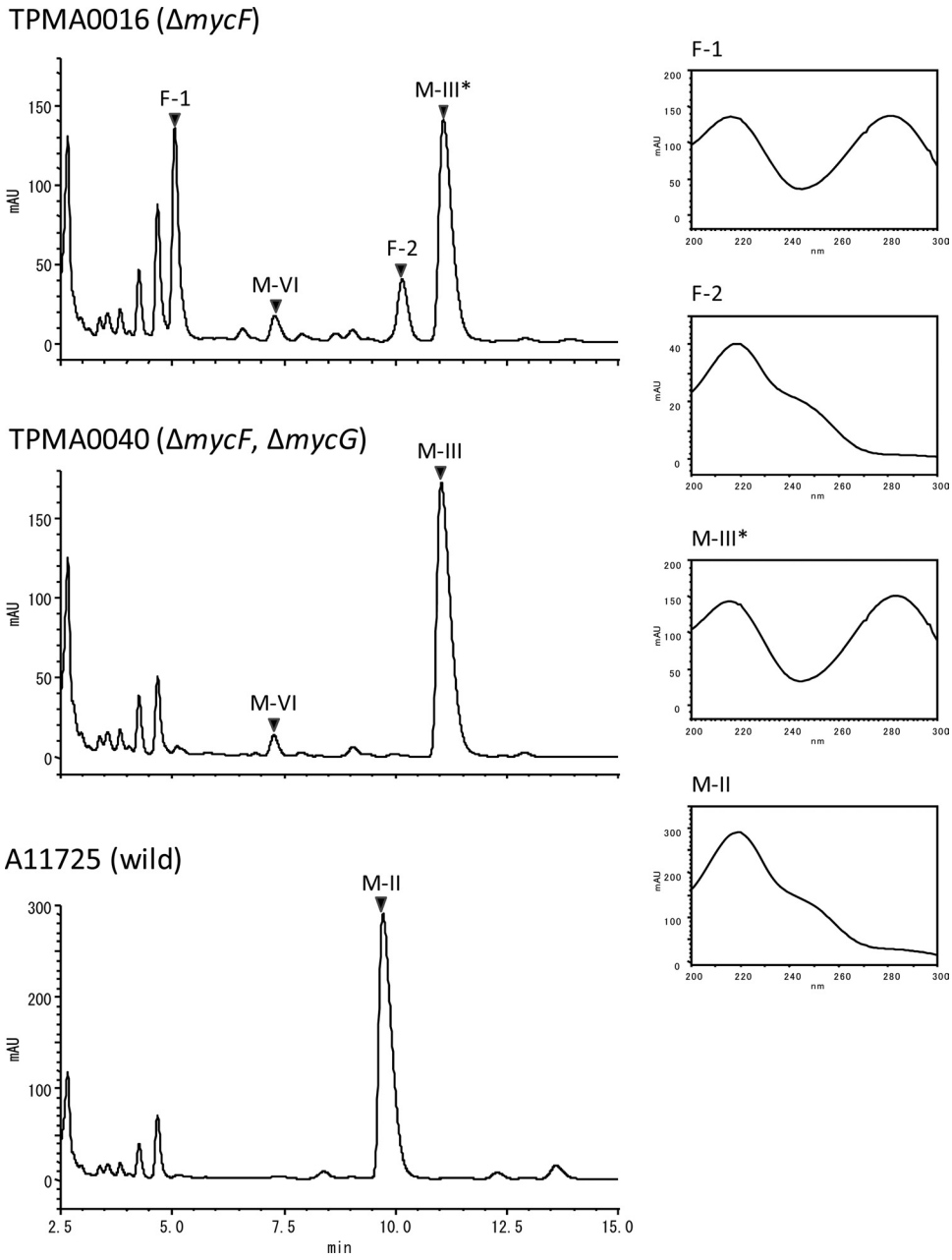

FIG 4 HPLC chromatograms (220 nm) of the EtOAc extracts obtained from the culture broths of the *mycF* disruption mutant TPMA0016, *mycF* and *mycG* double-disruption mutant TPMA0040, and the wild strain A11725 and UV spectrograms of M-II, M-III, F-1 (14-hydroxy-M-III, M-IX), and F-2 (12,13-epoxyl-M-III) on these chromatograms. HPLC conditions: column, ODS-80Tm (Tosoh, Japan); mobile phase, MeCN, 0.06% TFA (30:70); flow rate, 0.8 ml/min; UV wavelength, 200 to 300 nm.

TPMA0016 culture broth to obtain purified F-1 (12.6 mg) and F-2 (10.9 mg). The purified F-1 and F-2 were characterized by ^{1}H NMR (600 MHz) and ^{13}C NMR (150 MHz) spectroscopy. From their NMR chemical shifts (see Tables S2 and S3 in the supplemental material), molecular weight (*m/z* 698), and UV absorption spectra (Fig. 4), the structures of F-1 and F-2 were determined as C-14-hydroxy-M-III and C-12/13-epoxy-M-III, respectively. The ^{13}C NMR data for F-1 were almost the same as those for C-14-hydroxy-M-III, which was named mycinamicin IX (19); the ^{1}H NMR data for F-1 supported the structure. Moreover, the UV spectrum suggested the presence of an α,β-unsaturated lactone (216 nm) and an α,β,γ,δ-unsaturated ketone (281 nm). In contrast, the UV spectrum of F-2 suggested the presence of an α,β-unsaturated lactone (218 nm) and a γ,δ-epoxy-α,β-unsaturated ketone (240 nm). The chemical shifts of C-12 and C-13 were identical at 59.0 ppm, which was almost the same as those of M-I (59.6 ppm and 59.0 ppm, respectively), indicating an epoxide ring. Moreover, the chemical shift of C″3 was 69.5 ppm, which was almost the same as that of M-III (69.8 ppm), and the lack of the 2″-OCH_3 was also observed in the ^{1}H NMR and ^{13}C NMR spectra.

Therefore, F-2 was identified as C-12/13-epoxy-M-III, which was previously reported by Mierzwa et al. (23).

Antibacterial activities of C-14-hydroxy-M-III and C-12/13-epoxy-M-III were compared with those of M-III and M-IV (see Table S4 in the supplemental material). All tested compounds inhibited the growth of Gram-positive bacteria. MICs of C-12/13-epoxy-M-III were 0.20 μg/ml and 0.05 μg/ml against *S. aureus* ATCC 25923 and *M. luteus* ATCC 9341, respectively, and antibacterial activity of C-12/13-epoxy-M-III was as same as those of M-III and M-IV. However, the activity of C-14-hydroxy-M-III was lower than those of other tested compounds.

From the bioconversion study, we recognized that MycG converted M-IV into M-V and M-I and M-V into M-II in *M. griseorubida* but did not recognized M-I as a substrate. Moreover, the results of *mycF* and *mycG* double disruption indicated that M-III was also recognized as a substrate by MycG and that the MycG P450 protein catalyzes hydroxylation and also epoxidation at C-14 and C-12/13 on M-III in *M. griseorubida*. The results in this study support our previous enzymatic study using purified MycG proteins overexpressed in *E. coli* cells (4). MycG was previously shown to catalyze hydroxylation at the 6β-position of testosterone (1). Thus, MycG has a wide substrate specificity and multifunctional oxidation activity and plays an important role in the synthesis of mycinamicins by *M. griseorubida*.

ACKNOWLEDGMENTS

We are grateful to Akira Arisawa (Mercian Co., Japan) for donating pSAN-lac and Keith F. Chater (John Innes Centre, United Kingdom) for donating *E. coli* BW25113 and plasmids pIJ790, pIJ773, and pIJ776. We thank Shingo Fujisaki (Toho University) for help with LC-MS analysis and Wei Li (Toho University) for help with NMR spectroscopic analyses.

REFERENCES

1. **Agematu H, et al.** 2006. Hydroxylation of testosterone by bacterial cytochromes P450 using the *Escherichia coli* expression system. Biosci. Biotechnol. Biochem. **70**:307–311.
2. **Andersen JF, Hutchinson CR.** 1992. Characterization of *Saccharopolyspora erythraea* cytochrome P-450 genes and enzymes, including 6-deoxyerythronolide B hydroxylase. J. Bacteriol. **174**:725–735.
3. **Anzai Y, Ishii Y, Yoda Y, Kinoshita K, Kato F.** 2004. The targeted inactivation of polyketide synthase *mycAV* in the mycinamicin producer, *Micromonospora griseorubida*, and a complementation study. FEMS Microbiol. Lett. **238**:315–320.
4. **Anzai Y, et al.** 2008. Functional analysis of MycCI and MycG, cytochrome P450 enzymes involved in biosynthesis of mycinamicin macrolide antibiotics. Chem. Biol. **15**:950–959.
5. **Anzai Y, et al.** 2003. Organization of the biosynthetic gene cluster for the polyketide macrolide mycinamicin in *Micromonospora griseorubida*. FEMS Microbiol. Lett. **218**:135–141.
6. **Anzai Y, et al.** 2010. Isolation and characterization of 23-*O*-mycinosyl-20-dihydro-rosamicin: a new rosamicin analogue derived from engineered *Micromonospora rosaria*. J. Antibiot. **63**:325–328.
7. **Arisawa A, Tsunekawa H, Okamura K, Okamoto R.** 1995. Nucleotide sequence analysis of the carbomycin biosynthetic genes including the 3-*O*-acyltransferase gene from *Streptomyces thermotolerans*. Biosci. Biotech. Biochem. **59**:582–588.
8. **Baltz RH, Seno ET.** 1981. Properties of *Streptomyces fradiae* mutants blocked in biosynthesis of the macrolide antibiotic tylosin. Antimicrob. Agents Chemother. **20**:214–225.
9. **Bentley SD, et al.** 2002. Complete genome sequence of the model actinomycete *Streptomyces coelicolor* A3(2). Nature **417**:141–147.
10. **Bierman M, et al.** 1992. Plasmid cloning vectors for the conjugal transfer of DNA from *Escherichia coli* to *Streptomyces* spp. Gene **116**:43–49.
11. **Carlson JC, et al.** 2011. Tirandamycin biosynthesis is mediated by co-dependent oxidative enzymes. Nat. Chem. **3**:628–633.
12. **Coon MJ.** 2005. Cytochrome P450: nature's most versatile biological catalyst. Annu. Rev. Pharmacol. Toxicol. **45**:1–25.
13. **Guengerich FP.** 2001. Common and uncommon cytochrome P450 reactions related to metabolism and chemical toxicity. Chem. Res. Toxicol. **14**:611–650.
14. **Gust B, Challis GL, Fowler K, Kieser T, Chater KF.** 2003. PCR-targeted *Streptomyces* gene replacement identifies a protein domain needed for biosynthesis of the sesquiterpene soil odor geosmin. Proc. Natl. Acad. Sci. U. S. A. **100**:1541–1546.
15. **Hayashi M, et al.** 1981. Mycinamicins, new macrolide antibiotics. III Isolation and structures of mycinamicin aglycones, mycinolide IV and V. J. Antibiot. **34**:346–349.
16. **Ikeda H, et al.** 2003. Complete genome sequence and comparative analysis of the industrial microorganism *Streptomyces avermitilis*. Nat. Biotechnol. **21**:526–531.
17. **Inouye M, Takada Y, Muto N, Beppu T, Horinouchi S.** 1994. Characterization and expression of a P-450-like mycinamicin biosynthesis gene using a novel *Micromonospora-Escherichia coli* shuttle cosmid vector. Mol. Gen. Genet. **245**:456–464.
18. **Ishikawa J, et al.** 2004. The complete genomic sequence of *Nocardia farcinica* IFM 10152. Proc. Natl. Acad. Sci. U. S. A. **101**:14925–14930.
19. **Kinoshita K, Takenaka S, Suzuki H, Morohoshi T, Hayashi M.** 1992. Mycinamicins, new macrolide antibiotics. XIII. Isolation and structures of novel fermentation products from *Micromonospora griseorubida* (FERM BP-705). J. Antibiot. **45**:1–9.
20. **Kudo F, Motegi A, Mizoue K, Eguchi T.** 2010. Cloning and characterization of the biosynthetic gene cluster of 16-membered macrolide antibiotic FD-891: involvement of a dual functional cytochrome P450 monooxygenase catalyzing epoxidation and hydroxylation. Chembiochem **11**:1574–1582.
21. **Lamb DC, et al.** 2003. Cytochrome P450 complement (CYPome) of the avermectin-producer *Streptomyces avermitilis* and comparison to that of *Streptomyces coelicolor* A3(2). Biochem. Biophys. Res. Commun. **307**:610–619.
22. **Li S, Anzai Y, Kinoshita K, Kato F, Sherman DH.** 2009. Functional analysis of MycE and MycF, two *O*-methyltransferases involved in the biosynthesis of mycinamicin macrolide antibiotics. Chembiochem **10**:1297–1301.
23. **Mierzwa R, Truumees I, Patel M, Marquez J, Gullo V.** 1985. High-performance preparative isolation and purification of several mycinamicins. J. Liq. Chromatogr. **8**:1697–1709.
24. **Ohnishi Y, et al.** 2008. Genome sequence of the streptomycin-producing microorganism *Streptomyces griseus* IFO 13350. J. Bacteriol. **190**:4050–4060.
25. **Oliynyk M, et al.** 2007. Complete genome sequence of the erythromycin-producing bacterium *Saccharopolyspora erythraea* NRRL23338. Nat. Biotechnol. **25**:447–453.
26. **Richardson MA, Kuhstoss S, Solenberg P, Schaus NA, Rao RN.** 1987. A new shuttle cosmid vector, pKC505, for streptomycetes: its use in the cloning of three different spiramycin-resistance genes from a *Streptomyces ambofaciens* library. Gene **61**:231–241.
27. **Rix U, Fischer C, Remsing LL, Rohr J.** 2002. Modification of post-PKS tailoring steps through combinatorial biosynthesis. Nat. Prod. Rep. **19**:542–580.
28. **Rodriguez E, et al.** 2003. Rapid engineering of polyketide overproduction by gene transfer to industrially optimized strains. J. Ind. Microbiol. Biotechnol. **30**:480–488.
29. **Satoi S, Muto N, Hayashi M, Fujii T, Otani M.** 1980. Mycinamicins, new macrolide antibiotics. I. Taxonomy, production, isolation, characterization and properties. J. Antibiot. **33**:364–376.
30. **Stassi D, Donadio S, Staver MJ, Katz L.** 1993. Identification of a *Saccharopolyspora erythraea* gene required for the final hydroxylation step in erythromycin biosynthesis. J. Bacteriol. **175**:182–189.
31. **Tsukada S, et al.** 2010. Gene targeting for *O*-methyltransferase genes, *mycE* and *mycF*, on the chromosome of *Micromonospora griseorubida* producing mycinamicin with a disruption cassette containing the bacteriophage ϕC31 *attB* attachment site. FEMS Microbiol. Lett. **304**:148–156.
32. **Ward SL, et al.** 2004. Chalcomycin biosynthesis gene cluster from *Streptomyces bikiniensis*: novel features of an unusual ketolide produced through expression of the chm polyketide synthase in *Streptomyces fradiae*. Antimicrob. Agents Chemother. **48**:4703–4712.
33. **Xue Y, Wilson D, Zhao L, Liu Sherman H-WDH.** 1998. Hydroxylation of macrolactones YC-17 and narbomycin is mediated by the pikC-encoded cytochrome P450 in *Streptomyces venezuelae*. Chem. Biol. **5**:661–667.